Journal of Zhejiang University-SCIENCE A (Applied Physics & Engineering)
ISSN 1673-565X (Print); ISSN 1862-1775 (Online)
www.zju.edu.cn/jzus; www.springerlink.com
E-mail: jzus@zju.edu.cn

Screening study of transition metal oxide catalysts supported on ceria-modified titania for catalytic oxidation of toluene*

Dan-qing YU[1], Yue LIU[†‡1], Zhong-biao WU[1,2]

([1]*Department of Environmental Engineering, Zhejiang University, Hangzhou 310027, China*)

([2]*Zhejiang Provincial Engineering Research Center of Industrial Boiler & Furnace Flue Gas Pollution Control, Hangzhou 310027, China*)

[†]E-mail: yueliu@zju.edu.cn

Received July 6, 2010; Revision accepted Nov. 26, 2010; Crosschecked May 24, 2011

Abstract: Six transition metal oxides were added in ceria-modified titania using a sol-gel method for catalytic oxidation of toluene. An MnO*x* based catalyst was found to be the most active one, with which toluene could be decomposed completely at 200 ºC. The greatest Mn/Ti and molar ratio of the mobile oxygen to the total oxygen concentration, together with a large surface area and a low reduction peak-starting temperature, would result in its best activity in toluene oxidation.

Key words: Transition metal oxides, CeO_2/TiO_2, Sol-gel method, Catalytic oxidation, Toluene
doi:10.1631/jzus.A1000326 **Document code:** A **CLC number:** X511

1 Introduction

Volatile organic compounds (VOCs) are one major air contaminant released by industrial plants and transportation vehicles (Hinwood *et al*., 2007). Among the technologies for VOC abatement (absorption, adsorption, condensation, incineration, photocatalytic oxidation, and biodegradation, etc.), catalytic oxidation can efficiently decompose VOCs at much lower temperatures (300–500 ºC) than thermal incineration, saving energy consumption (Wang *et al*., 2009). The design of efficient catalysts is still a major challenge in achieving this goal.

Titania is one kind of support commonly used. Bertinchamps *et al*. (2006) found that titania based catalysts had performed better than those supported on different materials, including Al_2O_3 and SiO_2 in benzene oxidation. They also attributed the high activities to the promotion of homogeneous spreading of the active phase in the form of a monolayer. Furthermore, Krishnamoorthy *et al*. (2000) drew the conclusion that the difference between V_2O_5/Al_2O_3 and V_2O_5/TiO_2 catalysts lay in the interactions between vanadia and titania supports. This led to the different redox properties of vanadia, which resulted in the turnover frequency of o-dichlorobenzene (o-DCB) oxidation at 350 ºC of about one order of magnitude higher for the V_2O_5/Al_2O_3 counterpoint.

Ceria is a commercial material in catalytic applications, especially as a three-way catalyst. Since cerium has two stable oxidation states, Ce^{4+} and Ce^{3+}, oxygen could be transported via the redox cycle between Ce^{4+} and Ce^{3+}. The ceria doped catalysts exhibit improved oxygen mobilities, enhanced redox properties, and thus higher activity (Dai *et al*., 2008; Wang *et al*., 2009). In Xu *et al*. (2009), CeO_2/TiO_2 catalyst was very active in selective catalytic reduction of NO by NH_3.

As for the active phase, a great deal of effort has been made for various noble metal catalysts for their high activities (Avgouropoulos *et al*., 2006). Despite being less active than noble metals, transition metal oxides, much cheaper, better resistant in practical use,

‡ Corresponding author

* Project supported by Changjiang Scholar Incentive Program, Ministry of Education, China

and usually with a better thermal stability, have received considerable attention recently and have been considered as promising alternatives to noble metal catalysts for the catalytic oxidation of VOCs (Wu *et al.*, 2007; Wyrwalski *et al.*, 2007).

However, the investigated catalysts mentioned above were often prepared by the traditional impregnation method, which has the drawback that the active sites tend to aggregate during the evaporation of impregnated solutions, limiting the optimal loading content of active phases. Also the aggregated sites could cause the blockage of the porosity, preventing the reaction molecules from approaching the inner active phases (Li *et al.*, 2005). Comparatively, a sol-gel method would be beneficial to maintain a high specific surface area, controllable pore system, and good dispersion of the active phase, especially in the case of high loading (Kondo and Domen, 2008; Jiang *et al.*, 2009). Based on our former research results (Yu *et al.*, 2010), sol-gel-made CeO_2/TiO_2-based catalyst was more active than many other catalysts reported (Blanco *et al.*, 2007; Deng *et al.*, 2008; Huang *et al.*, 2008) under comparable operating conditions in toluene catalytic oxidation. This suggested that transition metal oxide supported on ceria-modified TiO_2 using the sol-gel method would be promising candidates in toluene catalytic oxidation.

However, to the best of our knowledge, a systematic investigation of this catalyst system was seldom undertaken. Therefore, in this paper, the sol-gel method was introduced to prepare several transition metal oxides (CrO*x*, MnO*x*, CuO, NiO*x*, CoO*x*, and FeO*x*) supported in Ce/TiO_2 and their catalytic behaviors were compared in low-temperature catalytic oxidation of toluene, an important persistent organic pollutant and a commonly used solvent in many industrial processes.

2 Experimental

2.1 Catalysts preparation

Tetrabutyl titanate, $Ti(OC_4H_9)_4$, acetic acid, ethanol, and water were mixed with a certain molar ratio under stirring to form a sol, and the molar ratio of precursor used was the optimal value obtained in our previous study for TiO_2 preparation (Wu *et al.*, 2007). Certain amounts of transition metal nitrate and cerium (III) nitrate hexahydrate were added during this process as M and Ce sources respectively. The M/Ti and Ce/Ti molar ratios were kept as 0.4 and 0.05 respectively according to the obtained results (Yu *et al.*, 2010). The sol transformed to gel after aging, and then it was dried and calcined. The obtained solids were crushed and sieved to 150–250 μm, and the sample was named MTC, where M represented the transition metal composition, e.g., CuTC. The pure TiO_2 and CeO_2/TiO_2 prepared with the same method were named T and TC, respectively.

2.2 Characterizations

The powder X-ray diffraction (XRD) patterns were obtained on a Rigaku D/MAX RA diffractometer (Rigaku, Japan) with an angle of 2θ from 20º to 80º. Nitrogen adsorption-desorption isotherms were obtained using a nitrogen adsorption apparatus (ASAP 2020, USA) at 77 K. The specific surface area was determined by the Brunauer-Emmett-Teller (BET) method, and pore volume and pore size of the samples were calculated by the Barrett-Jioner-Halenda (BJH) method. X-ray photoelectron spectroscopy (XPS) was performed using a Thermo ESCALAB 250 apparatus (USA) to investigate the surface chemical properties of the samples. Transmission electron microscopy (TEM) was applied to investigate the microstructures and particle sizes of the prepared samples with a JOEL JEM-2010 electron microscope (Japan). Temperature-programmed reduction of H_2 (H_2-TPR) were carried out using a custom-made setup equipped with thermal conductivity detector (TCD) with 50 mg catalysts to investigate the surface redox abilities of the catalysts, with the linear heating rate (5 ºC/min) in the same atmosphere from 100 to 800 or 900 ºC.

2.3 Catalytic activity test

The catalytic oxidation tests were carried out in a fixed bed reactor. The reactor was made of stainless-steel with an internal diameter of 9 mm and a height of 250 mm, in which 1 ml catalyst powder with the granulometric fraction of 150–250 μm was loaded. The reactor tube was located inside in a furnace which was electrically heated. The temperature was controlled with a type-K thermocouple, to maintain a stable bed temperature within ±1 ºC.

The feed gas (6% O_2 in nitrogen) with a

concentration of toluene of 1500 mg/m^3 was introduced to the catalyst bed with a total flow rate of 250 ml/min, to keep a constant gas hourly space velocity (GHSV) of 15000 h^{-1} for all studies. Before entering the reactor, the stream was blended in a static mixer (2 L), to eliminate the possible oscillations of initial toluene concentration. The temperature was lowered from 360 to 80 ºC in steps of 20–40 ºC, and the toluene conversions were examined after an appointed temperature was reached. A Fuli 9790 gas chromatograph (GC) (Fuli, China) equipped with a flame ionization detector (FID) was employed to analyze reactants and products. No other organic carbon-containing products were detected during the catalytic combustion of toluene. The activities of pure TiO_2 and CeO_2/TiO_2 were also examined for comparison.

3 Results and discussion

3.1 Catalytic performance for toluene oxidation

Fig. 1 presents the light-off curves of the supported transition metal oxide catalysts and the supports in the toluene oxidation. No obvious toluene conversion was observed over pure TiO_2 support (T) up to 200 ºC. After ceria modification (TC), the activity increased rapidly, and toluene conversion reached almost 80% at 360 ºC. When the transition metal oxide phases were introduced, the catalytic activities were enhanced significantly over the whole range of temperature investigated.

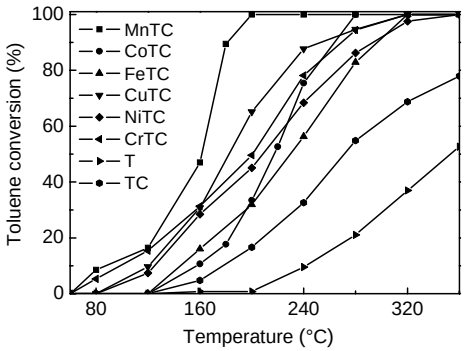

Fig. 1 Toluene light-off curves of the MO*x*-CeO_2/TiO_2 catalysts

The activities of the catalysts are ranked as follows based on the T_{50} (the temperature where 50% conversion is achieved): T (352 ºC)<TC (271 ºC)< FeTC (229 ºC)<CoTC (215 ºC)<NiTC (206 ºC)< CrTC (199 ºC)<CuTC (181 ºC)<MnTC (161 ºC). However the activity of CoTC increased faster, and outperformed the other catalysts with the exception of the MnTC catalyst in the high temperature range. The most active MnTC catalyst could oxidize toluene completely at 200 °C.

3.2 Textural properties of catalysts

Fig. 2 shows the XRD diagrams of the samples T and TC. The signals of anatase TiO_2 at 2θ=25.5º were detected in all XRD diagrams, while no evident diffraction peaks associated with ceria species appeared. After ceria addition, a large decrease of these peaks could be observed, which means that some strong interaction existed between ceria and titania, hindering the crystallization of TiO_2. A similar phenomenon was reported by Sinha and Suzuki (2005). The effect of dispersed titania phase which inhibits the agglomeration of the ceria phase, while the dispersion of titania nanocrystallites was also improved by the Ce-O-Ti type bonds.

The XRD diagrams of all the supported transition metal oxides samples were displayed in Fig. 3. A dramatic reduction of anatase phase signals occurred in all the transition-metal-oxide-contained catalysts. These phenomena were much more remarkable in the cases of MnTC, CoTC, and FeTC catalysts, implying that stronger interactions between the compositions might exist in these three samples.

All the transition metal oxide phases except MnO_x could be detected as bulk NiO, Co_3O_4, Fe_2O_3, CuO, and Cr_2O_3 crystallites respectively, which demonstrated that the manganese oxide phase

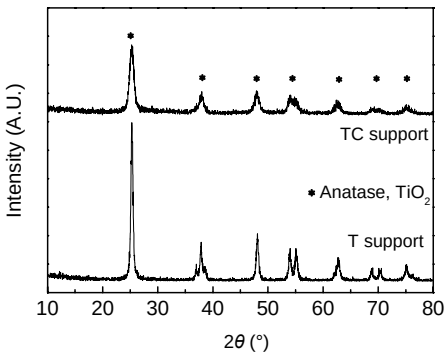

Fig. 2 X-ray diffraction patterns of the TiO_2 and CeO_2/TiO_2 supports

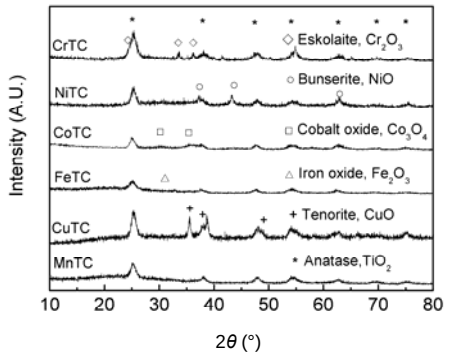

Fig. 3 X-ray diffraction patterns of the MO*x*-CeO_2/TiO_2 catalysts

dispersed better than the other active phases. However, considering their high loading content ((M/Ti=0.4), these relatively weak peaks associated with transition metal oxides implied that the oxide dispersion was improved because of the sol-gel method, the ceria modification, and the interaction between the compositions in MnTC catalyst.

As discussed above, the ceria modified titania support could effectively induce a good dispersion of the active phase at its surface, inhibiting the crystallite formation. Furthermore, Delimaris and Ioannides (2008) had found that the addition of manganese ions to ceria could help to control crystallite growth and to maintain the pore system of the materials, and vice versa. Similar phenomena were observed in the cases of Mn-Ce catalysts prepared by co-precipitation (Machida *et al.*, 2000; Qi *et al.*, 2004) and combustion methods (Murugan *et al.*, 2005), originated from the solid solution formation between Mn_2O_3 and CeO_2, because of their structural similarities. It was well recognized that the dispersion of the active phase played an important role in the oxidation reaction. This might explain the superior performance of MnTC compared with the other catalysts in toluene oxidation.

The specific surface area (S_{BET}), pore volume (V_p), and average pore radius (r_p) of the samples were determined by nitrogen adsorption-desorption, and listed in Table 1. The pure TiO_2 prepared by the sol-gel method had the smallest S_{BET} and V_p among the samples examined, and S_{BET} and V_p increased significantly after ceria modification. The inhibition of anatase phase crystallization by the added ceria as indicated in XRD would induce this change. After transition metal oxides addition, S_{BET} and V_p decreased slightly, except for the CrTC sample. Partial crystallization of some oxides would result in the S_{BET} and V_p drops. Combining with the XRD results, the highest crystallinity of copper oxide could reasonably explain its greatest reduction of V_p and r_p.

Table 1 Texture properties of the MO*x*-CeO_2/TiO_2 catalysts

Sample	S_{BET} (m^2/g)	V_p (cm^3/g)	r_p (nm)
T	32	0.05872	7.2
TC	118	0.298	10.0
MnTC	102	0.249	9.2
CoTC	107	0.189	6.9
CrTC	125	0.266	9.6
NiTC	101	0.230	9.8
FeTC	98	0.243	9.7
CuTC	67	0.208	5.9

Fig. 4 shows the TEM images of some selected catalysts. The well-crystallized anatase titania could be seen in all catalysts selected, while no CeO_2 crystalline could be observed. In the high-resolution transmission electron microscopy (HRTEM) of the CuTC sample (Fig. 4a), the CuO crystalline (whose lattice fringe is 0.218 nm, conforming to the ICDD-JCPDS database) could be observed clearly, accompanying the crystalline of anatase titania (whose lattice fringe is 0.348 nm). However, in the HRTEM images of CrTC and MnTC samples (not shown here), the crystallites of the transition metal oxides could not be detected. Calculated from the TEM images of the selected CrTC and MnTC (Figs. 4c and 4d) samples, the mean particle sizes of anatase titania particles are 7.8 and 10.8 nm, respectively (in accordance with the XRD results). The larger particle size of MnTC might be the reason for its relatively small S_{BET} and V_p compared with CrTC. Unlike the above mentioned two samples, the particle size of CuTC (Fig. 4b) was not well-distributed, and some large particles about 22–25 nm might be related to the crystallized CuO, which was in consistence with the XRD result (the mean diameter of CuO particle was determined to be 21.6 nm using the XRD pattern of CuTC). There are still some smaller grains (about 12.8 nm), which were considered as crystallized TiO_2. The formation of the large CuO particles would be the reason for its smallest S_{BET} and V_p among the catalysts investigated.

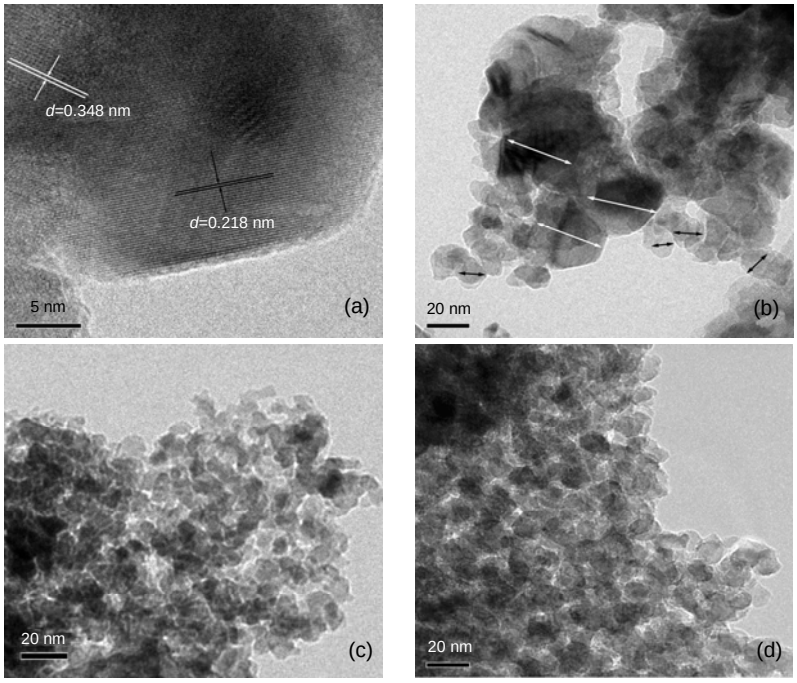

Fig. 4 High-resolution transmission electron microscopy (HRTEM) image of CuTC catalyst (a) and TEM images of CuTC (b), CrTC (c), and MnTC (d) catalysts
d: lattice fringe

3.3 X-ray photoelectron spectroscopy results

The chemical composition of the species and the oxidation states of the transition metal and the other elements contained on the catalyst surface were evaluated by XPS. The surface atomic ratios of Ce and M to Ti, the ratio of active oxygen to the total oxygen concentration, and the binding energies (BE) value of the main peak of metal elements are summarized in Table 2, and the O 1s scan spectra of the most active catalyst MnTC are presented in Fig. 5.

According to the peak binding energies of Fe, Co, Ni, and Cr (shown in Table 2), their oxidation states were mainly +3 (Alifanti *et al.*, 2006; Stoyanova *et al.*, 2006; Giraudon *et al.*, 2007; Oliveira *et al.*, 2008), which were consistent with the XRD results, except for the NiTC catalyst. However, the Cu 2p and Mn 2p profiles contained the peaks of Cu^{+} and Cu^{2+}, and Mn^{3+} and Mn^{4+} simultaneously (Peluso *et al.*, 2008; Yuan *et al.*, 2008), implying that mixed oxides or nonstoichiometric oxides existed in these samples. Their co-existences might be the result of crystal defects and distorted structures, accompanying higher amount of oxygen vacancies, stronger redox properties, and higher activities in toluene oxidation (Alvarez-Merino *et al.*, 2004). In these catalysts containing nonstoichiometric oxygen species, the adsorbed oxygen would have a different electronic structure, and the ionic character of their active oxygen species would increase, resulting in the improved catalytic behavior during oxidation (Pecchi *et al.*, 2008).

Table 2 X-ray photoelectron spectroscopy results of the MOx-CeO_2/TiO_2 catalysts with different main active phases

Sample	PE (eV)	M/Ti	Ce/Ti	O_A/O_{total}
TC	–	–	0.149	0.137
FeTC	711.0	0.467	0.153	0.152
CoTC	780.7	0.492	0.189	0.165
NiTC	855.9	0.463	0.148	0.172
CrTC	576.7	0.516	0.205	0.182
CuTC	933.0	0.549	0.197	0.179
MnTC	641.3	0.578	0.212	0.191

PE: peak binding energy of transition metals; O_A/O_{total}: molar ratio of the active oxygen to the total oxygen concentration; M/Ti and Ce/Ti: surface molar ratios of Ce and M to Ti, respectively

The O 1s profile can be deconvoluted into three contributions referred to as the chemisorbed oxygen species at 531–531.7 eV (denoted as O_A), the lattice oxygen at 529.5–530.1 eV (O_B), and absorbed oxygen

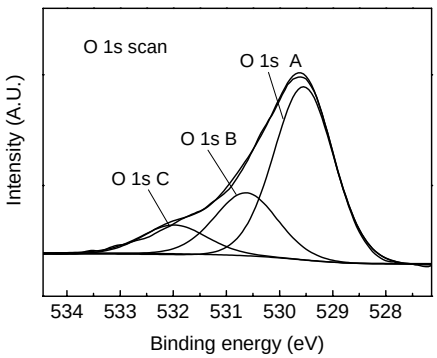

Fig. 5 O 1s X-ray photoelectron spectroscopy spectra profiles of the MnTC catalysts

species present at 531.9–532.9 eV (O_C). The O_A species were considered to be active oxygen species and could play important roles in oxidation reactions (Niu *et al.*, 2007; Wang *et al.*, 2009), so O_A/O_{total} ratio listed in Table 2 was used as an index to represent the vigorous oxidative capacity of a certain catalyst. As shown in Table 2, the ceria-contained sample, TC already had a considerable amount of active oxygen, but the addition of transition metal oxides could increase the ratio further. The superficial O_A/O_{total} ratio of the most active catalyst, MnTC, was higher than those of any other catalysts examined. As expected, ceria is a kind of material with good oxygen storage capacity, and there existed a synergistic mechanism between the manganese oxide and ceria according to the results of Qi *et al.* (2004). Oxygen could be transported through the redox cycle between the valence variation of manganese and cerium oxides. Therefore, the ceria modification and the stronger interaction between the compositions also contribute to the more superficial active oxygen species of this sample.

The nominal molar ratio of M/Ti in the preparation process was kept as 0.4. Then the increase of M/Ti detected by XPS shows an improved enrichment of MO*x* phase on the surface of support, leading to higher activity in oxidation reaction, while a smaller M/Ti ratio indicates that more active phase sites migrated from surface to bulk. Furthermore, it could be observed that the three most active catalysts, CrTC, CuTC, and MnTC had larger M/Ti ratios than the more inert catalysts, FeTC, CoTC, and NiTC (Table 2). Then it could be concluded that the dispersion and enrichment of active phase (expressed by M/Ti) on the surface play a vital role in catalytic oxidation process. It was noted that the absence of XRD signals from active phase and the largest M/Ti ratio occurred in the most active MnTC catalyst simultaneously.

3.4 Results of temperature-programmed reduction of H_2

The TPR profiles are presented to investigate the redox capacities of the catalysts concerned (Fig. 6).

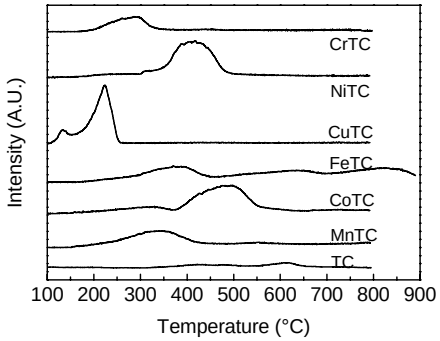

Fig. 6 Temperature-programmed reduction of H_2 patterns of the catalysts with different main active phases

The ceria modified titania support displayed only a very weak reduction peak above 600 °C, while after the addition of the transition metal oxide active phase, the redox capacities of all the samples were improved significantly. Among the six catalysts prepared, the two most active ones, MnTC and CrTC, had lower peak-starting temperatures, while for the less active three, NiTC, CoTC, and FeTC, the reduction peaks started at higher temperatures, which indicated their lattice oxygen would be more difficult to activate. The CuTC catalyst had a much lower peak-starting temperature than the other catalysts, because of the readiness of CuO*x* reducibility, which was consistent with Ribeiro *et al.* (2007).

The two reduction peaks of the CuTC catalyst in series corresponded to the reduction of CuO to Cu_2O, then partially to metal Cu (Tidahy *et al.*, 2007). The first peak was small, implying that the CuO*x* contained was the mixture of CuO and Cu_2O, as revealed by the XPS results. The TPR result showed that this catalyst had a superior redox capacity than the other MO*x*-CeO_2/TiO_2 catalysts. However, considering its poor textural properties (small specific surface area and pore volume) and the high crystallinity of CuO particles (supported by the intense XRD signals and

TEM image), this catalyst was less active in toluene oxidation than the MnTC catalyst, and even less active than the NiTC catalyst in the high temperature range.

The most inactive catalyst, FeTC showed three consecutive peaks at very high temperatures, and all the three peaks were relatively weak. This would explain its poor behavior in toluene oxidation.

The most active catalyst, MnTC exhibited a broad peak spanned between 160–450 ºC, which was associated with the successive reduction steps: amorphous $Mn_2O_3 \rightarrow Mn_3O_4 \rightarrow MnO$ (Gutierrez-Ortiz *et al.*, 2007). It was reported that a commercial manganese oxide, Mn_2O_3 had one peak at 490 ºC and the other of Mn_3O_4 at 520 ºC (Delimaris and Ioannides, 2008). The lower peak temperature might be attributed to the ceria modification and the high dispersion of manganese oxide on the surface. This sample did not show an obviously superior behavior to the other catalysts in H_2-TPR examination. Delimaris and Ioannides (2008) had observed a similar result, and attributed this variation to the fact that the reducing agent under reaction conditions is the more complicated VOC molecule, rather than H_2 as in TPR. Many other complicated factors involved could explain the difference between the dissatisfactory H_2-TPR behavior and the highest activity in real toluene oxidation of MnTC.

From the H_2-TPR results, it could be concluded that the reduction peak-starting temperature, which corresponded to the feasibility of the lattice oxygen activation, was more associated with the catalytic performances than the reduction peak intensity, which reflected the amount of lattice oxygen that could be reduced. This could explain the consistency between the lower reduction peak-starting temperature and the superior behavior in toluene complete oxidation of the MnTC catalyst.

4 Conclusions

Six types transition metal oxides (CrO*x*, MnO*x*, CoO*x*, CuO*x*, FeO*x*, and NiO*x*) were added in CeO_2/TiO_2 using a sol-gel method, and their behaviors in toluene oxidation were investigated.

The catalysts activities in catalytic oxidation of toluene are ranked in the following sequence (based on the T_{50}): T<TC<FeTC<CoTC<NiTC<CrTC<CuTC<MnTC. The most active catalyst, MnTC, could decompose toluene completely at 200 ºC.

XRD characterization demonstrated a good dispersion of the active phases for all the samples with the exception of CuTC. The XPS investigation showed that the enrichment of active phases and mobile oxygen species would be obtained, contributing to the good performances in toluene oxidation. These were the integrated results of the sol-gel method and ceria modification.

The peak intensity of H_2-TPR could not be directly associated with the catalytic activity, but the reduction peak-starting temperature reflected the catalytic performance to a certain extent. For example, CuTC, which had the most intense TPR peaks at very low temperatures, did not perform very well in toluene oxidation, due to the much higher crystallinity of CuO and a much smaller surface area.

A considerably larger surface area, a lower reduction peak-starting temperature, the largest Mn/Ti and molar ratio of the mobile oxygen to the total oxygen concentration, and the existence of non-stoichiometric oxides could be the most important causes of the superior behavior of the MnTC catalyst in toluene oxidation.

References

Alifanti, M., Florea, M., Cortes-Corberan, V., Endruschat, U., Delmon, B., Parvulescu, V.I., 2006. Effect of $LaCoO_3$ perovskite deposition on ceria-based supports on total oxidation of VOC. *Catalysis Today*, **112**(1-4):169-173. [doi:10.1016/j.cattod.2005.11.017]

Alvarez-Merino, M.A., Ribeiro, M.F., Silva, J.M., Carrasco-Marian, F., Maldonado-Hodar, F.J., 2004. Activated carbon and tungsten oxide supported on activated carbon catalysts for toluene catalytic combustion. *Environmental Science & Technology*, **38**(17):4664-4670. [doi:10.1021/es034964c]

Avgouropoulos, G., Oikonomopoulos, E., Kanistras, D., Ioannides, T., 2006. Complete oxidation of ethanol over alkali-promoted Pt/Al_2O_3 catalysts. *Applied Catalysis B: Environmental*, **65**(1-2):62-69. [doi:10.1016/j.apcatb.2005.12.016]

Bertinchamps, F., Gregoire, C., Gaigneaux, E.M., 2006. Systematic investigation of supported transition metal oxide based formulations for the catalytic oxidative elimination of (chloro)-aromatics: Part I: Identification of the optimal main active phases and supports. *Applied Catalysis B: Environmental*, **66**(1-2):1-9. [doi:10.1016/j.apcatb.2006.02.011]

Blanco, J., Petre, A.L., Yates, M., Martin, M.P., Martn, J.A.,

Martin-Luengo, M.A., 2007. Tailor-made high porosity VOC oxidation catalysts prepared by a single-step procedure. *Applied Catalysis B: Environmental*, **73**(1-2): 128-134. [doi:10.1016/j.apcatb.2006.06.017]

Dai, Q.G., Wang, X.Y., Lu, G.Z., 2008. Low-temperature catalytic combustion of trichloroethylene over cerium oxide and catalyst deactivation. *Applied Catalysis B: Environmental*, **81**(3-4):192-202. [doi:10.1016/j.apcatb.2007.12.013]

Delimaris, D., Ioannides, T., 2008. VOC oxidation over MnO*x*-CeO_2 catalysts prepared by a combustion method. *Applied Catalysis B: Environmental*, **84**(1-2):303-312. [doi:10.1016/j.apcatb.2008.04.006]

Deng, J.G., Zhang, L., Dai, H.X., He, H., Au, C.T., 2008. Strontium-doped lanthanum cobaltite and manganite: highly active catalysts for toluene complete oxidation. *Industrial & Engineering Chemistry Research*, **47**(21): 8175-8183. [doi:10.1021/ie800585x]

Giraudon, J.M., Elhachimi, A., Wyrwalski, F., Siffert, S., Aboukais, A., Lamonier, J.F., Leclercq, G., 2007. Studies of the activation process over Pd perovskite-type oxides used for catalytic oxidation of toluene. *Applied Catalysis B: Environmental*, **75**(3-4):157-166. [doi:10.1016/j.apcatb.2007.04.005]

Gutierrez-Ortiz, J.I., Rivas, B., Lopez-Fonseca, R., Martín, S., Gonzalez-Velasco, J.R., 2007. Structure of Mn-Zr mixed oxides catalysts and their catalytic performance in the gas-phase oxidation of chlorocarbons. *Chemosphere*, **68**(6):1004-1012. [doi:10.1016/j.chemosphere.2007.02.025]

Hinwood, A.L., Rodriguez, C., Runnion, T., Farrar, D., Murray, F., Horton, A., Glass, D., Sheppeard, V., Edwards, J.W., Denison, L., *et al*., 2007. Risk factors for increased BTEX exposure in four Australian cities. *Chemosphere*, **66**(3):533-541. [doi:10.1016/j.chemosphere.2006.05.040]

Huang, H.F., Liu, Y.Q., Tang, W., Chen, Y.F., 2008. Catalytic activity of nanometer $La_{1-x}Sr_xCoO_3$ (x=0, 0.2) perovskites towards VOCs combustion. *Catalysis Communications*, **9**(1):55-59. [doi:10.1016/j.catcom.2007.05.004]

Jiang, B.Q., Liu, Y., Wu, Z.B., 2009. Low-temperature selective catalytic reduction of NO on MnO*x*/TiO_2 prepared by different methods. *Journal of Hazardous Material*, **162**(1):1249-1254. [doi:10.1016/j.jhazmat.2008.06.013]

Kondo, J.N., Domen, K., 2008. Crystallization of mesoporous metal oxides. *Chemical Material*, **20**(3):835-847. [doi:10.1021/cm702176m]

Krishnamoorthy, S., Rivas, J.A., Amiridi, M.D., 2000. Catalytic oxidation of 1,2-dichlorobenzene over supported transition metal oxides. *Journal of Catalysis*, **193**(2): 264-272. [doi:10.1006/jcat.2000.2895]

Li, J.J., Xu, X.Y., Jiang, Z., Hao, Z.P., Hu, C., 2005. Nanoporous silica-supported nanometric palladium: synthesis, characterization, and catalytic deep oxidation of benzene. *Environmental Science and Technology*, **39**(5):1319-1323. [doi:10.1021/es0491174]

Machida, M., Uto, M., Kurogi, D., Kijima, T., 2000. MnO*x*-CeO_2 binary oxides for catalytic NO*x* sorption at low temperatures. sorptive removal of NO*x*. *Chemical Material*, **12**(10):3158-3164. [doi:10.1021/cm000207r]

Murugan, B., Ramaswamy, A.V., Srinivas, D., Gopinath, C.S., Ramaswamy, V., 2005. Nature of manganese species in $Ce_{1-x}Mn_xO_{2-\delta}$ solid solutions synthesized by the solution combustion route. *Chemical Material*, **17**(15):3983-3993. [doi:10.1021/cm050401j]

Niu, J.R., Deng, J.G., Liu, W., Zhang, L., Wang, G.Z., Dai, H.X., He, H., Zi, X.H., 2007. Nanosized perovskite-type oxides $La_{1-x}Sr_xMO_{3-\delta}$ (M=Co, Mn; x=0, 0.4) for the catalytic removal of ethylacetate. *Catalysis Today*, **126**(3-4):420-429. [doi:10.1016/j.cattod.2007.06.027]

Oliveira, L.C.A., Lago, R.M., Fabris, J.D., Sapag, K., 2008. Catalytic oxidation of aromatic VOCs with Cr or Pd-impregnated Al-pillared bentonite: byproduct formation and deactivation studies. *Applied Clay Science*, **39**(3-4): 218-222. [doi:10.1016/j.clay.2007.06.003]

Pecchi, G., Reyes, P., Zamora, R., Cadus, L.E., Fierro, J.L.G., 2008. Surface properties and performance for VOCs combustion of $LaFe_{1-y}Ni_yO_3$ perovskite oxides. *Journal of Solid State Chemistry*, **181**(4):905-912. [doi:10.1016/j.jssc.2008.01.020]

Peluso, M.A., Gambaro, L.A., Pronsato, E., Gazzoli, D., Thomas, H.J., Sambeth, J.E., 2008. Synthesis and catalytic activity of manganese dioxide (type OMS-2) for the abatement of oxygenated VOCs. *Catalysis Today*, **133-135**:487-492. [doi:10.1016/j.cattod.2007.12.132]

Qi, G.S., Yang, R.T., Chang, R., 2004. MnO*x*-CeO_2 mixed oxides prepared by co-precipitation for selective catalytic reduction of NO with NH_3 at low temperatures. *Applied Catalysis B: Environmental*, **51**(2):93-106. [doi:10.1016/j.apcatb.2004.01.023]

Ribeiro, M.F., Silva, J.M., Brimaud, S., Antunes, A.P., Silva, E.R., Fernandes, A., Magnoux, P., Murphy, D.M., 2007. Improvement of toluene catalytic combustion by addition of cesium in copper exchanged zeolites. *Applied Catalysis B: Environmental*, **70**(1-4):384-392. [doi:10.1016/j.apcatb.2006.01.027]

Sinha, A.K., Suzuki, K., 2005. Preparation and characterization of novel mesoporous ceria-titania. *Jounal of Physical Chemistry B*, **109**(5):1708-1714. [doi:10.1021/jp046391b]

Stoyanova, M., Konova, P., Nikolov, P., Naydenov, A., Christoskova, S., Mehandjiev, D., 2006. Alumina-supported nickel oxide for ozone decomposition and catalytic ozonation of CO and VOCs. *Chemical Engineering Journal*, **122**(1-2):41-46. [doi:10.1016/j.cej.2006.05.018]

Tidahy, H.L., Siffert, S., Wyrwalski, F., Lamonier, J.F., Aboukais, A., 2007. Catalytic activity of copper and palladium based catalysts for toluene total oxidation. *Catalysis Today*, **119**(1-4):317-320. [doi:10.1016/j.cattod.2006.08.02]

Wang, X.Y., Kang, Q., Li, D., 2009. Catalytic combustion of chlorobenzene over MnO*x*-CeO_2 mixed oxide catalysts. *Applied Catalysis B: Environmental*, **86**(3-4):166-175. [doi:10.1016/j.apcatb.2008.08.009]

Wu, Z.B., Jiang, B.Q., Liu, Y., Zhao, W.R., Guan, B.H., 2007. Experimental study on a low-temperature SCR catalyst based on MnO*x*/TiO_2 prepared by sol-gel method. *Journal of Hazardous Materials*, **145**(3):488-494. [doi:10.1016/j.jhazmat.2006.11.045]

Wyrwalski, F., Lamonier, J.F., Siffert, S., Aboukais, A., 2007. Additional effects of cobalt precursor and zirconia support modifications for the design of efficient VOC oxidation catalysts. *Applied Catalysis B: Environmental*, **70**(1-4):393-399. [doi:10.1016/j.apcatb.2006.01.023]

Xu, W.Q., He, H., Yu, Y.B., 2009. Deactivation of a Ce/TiO_2 catalyst by SO_2 in the selective catalytic reduction of NO by NH_3. *Journal of Physical Chemistry C*, **113**(11):4426-4432. [doi:10.1021/jp8088148]

Yu, D.Q., Liu, Y., Wu, Z.B., 2010. Low temperature catalytic oxidation of toluene over mesoporous MnO*x*-CeO_2/TiO_2 prepared by sol-gel method. *Catalysis Communications*, **11**(8):788-791. [doi:10.1016/j.catcom.2010.02.016]

Yuan, S.H., Shen, M., Gong, M.C., Wang, J.L., Yan, S.H., Cao, H.Y., Chen, Y.Q., 2008. Catalytic combustion of ethyl acetate over Al_2O_3-$Ce_{0.5}Zr_{0.5}O_2$ supported metal oxide catalysts. *Acta Physico-Chimica Sinica*, **24**(3):364-368. [doi:10.1016/S1872-1508(08)60015-7]